Applied Microbiology and Biotechnology (2024) 108:15
https://doi.org/10.1007/s00253-023-12891-9

BIOTECHNOLOGICAL PRODUCTS AND PROCESS ENGINEERING

Fermentation of waste water from agar processing with *Bacillus subtilis* by metabolomic analysis

Yanyan Wu[1] · Boyan Duan[1] · Qiaoyan Lin[1] · Yingying Liang[1] · Xiping Du[1,2,3] · Mingjing Zheng[1,2,3] · Yanbing Zhu[1,2,3] · Zedong Jiang[1,2,3] · Qingbiao Li[1,2,3] · Hui Ni[1,2,3,4] · Zhipeng Li[1,2,3] · Jinfang Chen[1,5]

Received: 3 July 2023 / Revised: 1 November 2023 / Accepted: 22 November 2023

Abstract

Fungal infection has become a major threat to crop loss and affects food safety. The waste water from agar processing industries extraction has a number of active substances, which could be further transformed by microorganisms to synthesize antifungal active substances. In this study, *Bacillus subtilis* was used to ferment the waste water from agar processing industries extraction to analyze the antifungal activity of the fermentation broth on *Alternaria alternata* and *Alternaria* spp. Results showed that 25% of the fermentation broth was the most effective in inhibited *A. alternata* and *Alternaria* spp., with fungal inhibition rates of 99.9% and 96.1%, respectively, and a minimum inhibitory concentration (MIC) was 0.156 μg/mL. Metabolomic analysis showed that flavonoid polyphenols such as coniferyl aldehyde, glycycoumarin, glycitin, and procyanidin A1 may enhance the inhibitory activity against the two pathogenic fungal strains. Kyoto Encyclopedia of Genes and Genomes (KEGG) analysis showed that polyphenols involved in the biosynthesis pathways of isoflavonoid and phenylpropanoid were upregulated after fermentation. The laser confocal microscopy analyses and cell conductivity showed that the cytoplasm of fungi treated with fermentation broth was destroyed. This study provides a research basis for the development of new natural antifungal agents and rational use of seaweed agar waste.

Key points

- *Bacillus subtilis fermented waste water has antifungal activity*
- *Bacillus subtilis could transform active substances in waste water*
- *Waste water is a potential raw material for producing antifungal agents*

Keywords *Bacillus subtilis* · *Alternaria alternata* · *Alternaria* spp. · Seaweed waste water · Antifungal activity

Introduction

Post-harvest loss of fruits and vegetables has become a major threat to food security (Wang et al. 2023). Microbial infection is the main cause of food spoilage, so effectively controlling the growth and reproduction of plant pathogens is the key to solving the post-harvest losses of fruits and vegetables (Wang et al. 2022). *Alternaria* species is one of the most common foliar pathogens and a susceptible pathogenic fungus for crops, such as tomatoes and apples (Wang et al. 2022). Although chemical fungicides can effectively prevent and control microbial diseases, long-term use will affect the environment and human body (Duan et al. 2021). Therefore, new natural biological agents should be developed.

Bacillus subtilis is a group of aerobic, Gram-positive bacteria (Lin et al. 2020) and has significant antifungal activity and resistance to stress; this species is therefore widely used

✉ Zhipeng Li
lzp2019@jmu.edu.cn

✉ Jinfang Chen
jfchen@jmu.edu.cn

1 College of Ocean Food and Biological Engineering, Jimei University, Xiamen 361021, Fujian, China

2 Fujian Provincial Key Laboratory of Food Microbiology and Enzyme Engineering, Xiamen 361021, Fujian, China

3 Research Center of Food Biotechnology of Xiamen City, Xiamen 361021, Fujian, China

4 Xiamen Ocean Vocational College, Xiamen 361021, Fujian, China

5 College of Harbour and Coastal Engineering, Jimei University, Xiamen 361021, Fujian, China

Published online: 03 January 2024

in agricultural biological control and plant growth promotion (Ma et al. 2015; Gao et al. 2018). Berlanga-Clavero et al. found that *B. subtilis* could metabolize the fungus-inhibiting lipopeptide fengycin and inhibit the growth of *Staphylococcus griseus*; as such, *B. subtilis* could be used to control the foliar fungus gray mold of melon (Berlanga-Clavero et al. 2022). Li et al. isolated a potential endophytic *B. subtilis* L1-21 from citrus; the fermentation filtrate showed good biological control of citrus green mold and contained potential fungal inhibitory compounds such as surfactin, fengycin, bacillaene, and bacilysin (Li et al. 2022a). Ali et al. found that the application of *B. subtilis* culture filtrate to the leaf surface reduced the size and frequency of spots caused by *Alternaria alternata* by 68 to 81% (Ali et al. 2016).

Seaweed gum from *Gracilaria* is a common food colloid, and the extraction process produces a large amount of waste liquid containing organic active substances. Active substances derived from seaweed can be used to synthesize antifungal active polyphenols through the transformation of microorganisms. Therefore, waste water from agar processing industries fermented by *B. subtilis* could be used to develop and synthesize antifungal active substances. However, the mechanism through which the fermentation of *B. subtilis* transforms the agar waste into antifungal substances remains unclear. In this regard, the mechanism of the synthesis of antifungal active substances after the fermentation of *B. subtilis* with waste water from agar processing industries should be investigated.

In this study, *B. subtilis* was used as a seed in fermentation with waste water from agar processing industries as the carbon and nitrogen source in the medium. The inhibitory activity of the fermentation supernatant against *A. alternata* and *Alternaria* spp. was determined using mycelial growth inhibition rate and minimum inhibitory concentration (MIC). The contents of the main active ingredients in the fermentation supernatant were measured. Metabolomics was used to screen metabolic differentials in the fermentation supernatant and identify inhibitory substances. Laser confocal microscopy staining and conductivity test were used to explore the antifungal mechanism of the metabolites. The research about process and mechanism of producing antifungal active substances through microbial fermentation of waste water from agar processing industries was explored, which provides a research basis for the extraction of seaweed waste resources.

Materials and methods

Raw materials and strains

Waste water from agar processing industries was provided by GreenFresh (Fujian) Food Co., Ltd. (Fujian, China). *B. subtilis* (ATCC 6633) was purchased from the China Center for the Conservation and Management of Pharmaceutical Microbial Strains. *A. alternata* (BNCC 336535) was obtained from Henan Industrial Microbial Strain Engineering Technology Research Center (Henan, China). *Alternaria* spp. (BNCC 123548) was acquired from Henan Industrial Microbial Strain Engineering Technology Research Center (Henan, China).

Activation of *B. subtilis*

B. subtilis was inoculated into 100 mL LB liquid medium at an inoculum volume of 2% and cultured under shaken at 37 °C and 180 rpm/min for 18 h. Culture of *B. subtilis* was used as seed liquid when the OD_{600} value reached 0.6 − 0.7.

Preparation of waste water from agar processing industries as fermentation medium

The agar extraction process involves four steps: alkali treatment, acid treatment, bleaching, and gel boiling. After alkaline treatment of seaweed, it was necessary to repeatedly rinse it with a large amount of water until it becomes neutral. This would produce a large amount of alkali waste water. Similarly, a large amount of waste water would also be produced during acid treatment and bleaching. The picture of the waste water was shown in (Fig. S1A). The COD value of waste water from agar processing industries was measured by a chemical oxygen demand (COD) rapid measuring instrument is 85 g/L. The pH of waste water required for the experiment was adjusted from 14.1 to 7.2–7.4.

Waste water was used to replace the yeast extract and tryptone in the LB liquid medium (tryptone 50%, yeast extract 25%, and sodium chloride 25%) as the carbon and nitrogen source. According to the COD value (85 g/L), pretreated waste water, yeast extract, and tryptone were used to prepare waste water culture medium containing 0%, 25%, 50%, 75%, and 100% according to the proportion of carbon and nitrogen source. The required sodium chloride was added to obtain 150 mL of fermentation medium for the experimental system in a 500 mL Erlenmeyer flask. Then, 1 mol/L hydrochloric acid was added to adjust the pH to 7.2 ± 0.2.

Fermentation of waste water from agar processing industries

B. subtilis seed liquid was inoculated in LB liquid medium at 5% inoculum and incubated at 37 ℃ and 180 rpm/min in an incubator for 72 h to obtain fermentation broth. The picture of the fermentation broth was shown in (Fig. S1B). The fermentation broth was centrifuged at 8000 rpm/min for 30 min in a high-speed freezing centrifuge (Eppendorf,

Germany). The supernatant was filtered through a 0.22 μm membrane to remove bacteria.

Determination of the antifungal activity of waste water from agar processing industries before and after fermentation with *B. subtilis*

Fungal inhibition was evaluated using mycelial growth inhibition rate (Zhang et al. 2017). Then, 50 mL of pre- and post-fermentation broth was collected and centrifuged in a high-speed refrigerated centrifuge at 8000 rpm/min for 30 min. The supernatant was filtered and sterilized with a 0.22 μm aqueous filter membrane in the ultra-clean stage. About 10 mL of the supernatant of different samples was added to 90 mL of PDA medium as the experimental group, while the same volume of sterile water was used as the blank control group and 25 mg/L amphotericin B was used as the positive control group to prepare drug-containing plates (90 mm) at a final concentration of 10% (v/v). Three parallel sets of samples were set up for each group. *A. alternata* (BNCC 336535) and *Alternaria* spp. (BNCC 123548) mycelium blocks with a diameter of 6 mm were respectively inoculated into the center of the drug-containing plate and incubated at 28 ℃ until the mycelium of the blank control group had grown over the entire plate. The diameter of the colony in each experimental group and the control group was measured by cross method (Mi et al. 2023; Admassie et al. 2022). The growth inhibition rate of mycelia was calculated by the following formula:$i = (1 - \frac{Ax}{A0}) \times 100$, where *i* was the growth inhibition rate of mycelia, *A*0 was the hyphal diameter of the untreated pathogen, and Ax was the hyphal diameter of the treated pathogen (Li et al. 2021a).

Determination of MIC of fermented crude extracts against *A. alternata* and *Alternaria* spp.

The fermented supernatant was freeze-dried in a vacuum freeze dryer to obtain a powdered sample of the fermented crude extract. About 10 mL of sterile water, 25 mg/L amphotericin B, and fermented crude extracts (at concentrations of 2.500, 1.250, 0.625, 0.313, 0.156, 0.078, and 0.039 μg/mL) were added to 90 mL of PDA medium as blank control group, positive control group, and experimental groups. Three parallel sets of samples were set up for each group. A 6-mm diameter block was inoculated in the center of the drug-containing plate (90 mm) and incubated at 28 ℃ until the mycelium of the blank control group had grown over the entire plate. The diameter of the microsphere in each experimental group and the control group was measured by cross method. The growth inhibition rate of mycelia was calculated by the following formula: $i = (1 - \frac{Ax}{A0}) \times 100$, where *i* was the growth inhibition rate of mycelia, *A*0 was the hyphal diameter of the untreated pathogen, and Ax was the hyphal diameter of the treated pathogen (Li et al. 2021a).

Metabolomics identification of primary metabolites in fermented waste water from agar processing industries

The fermentation broth samples before and after fermentation of the 25% waste water group were taken out, thawed, eddied for 10 s, and centrifuged at 4 ℃ for 20 min at 12,000 rpm/min. About 1 mL of the supernatant was collected and diluted 50,000 times with ultrapure water to obtain a sample concentration of below 1 ppm. The diluted sample (400 μL) was added to 100 μL of 1 ng/μL astaxanthin as an internal standard and eddied for 10 s through a 0.22 μm aqueous microporous filter membrane.

Metabolite analysis was performed on an ACQUITY Ultra Performance Liquid Chromatography I-Class PLUS system (Waters, Milford, USA) and a Xevo G0-XS TOF mass spectrometer (Waters, Milford, USA) equipped with an ESI source. MS-DIAL 4.80 software with a public database (http://prime.psc.riken.jp/compms/msdial/main.html#MSP) was used for analysis. Substances were compared with databases using their secondary mass spectrometry information. Duplicate signals of K^+, Na^+, and NH_4^+ were removed during the analysis. Metabolite quantification was accomplished using triple quadrupole mass spectrometry in full information tandem mass spectrometry scanning mode (MS^E). The integration and correction of the peaks of the same metabolite in different samples was conducted using the characteristic peaks of the six standards available in the laboratory.

Liquid chromatography parameters: ACQUITY UPLC BEH C18 column (2.1 mm × 50 mm, 1.7 μm, Waters, Milford, USA) was selected. Mobile phase A was ultrapure water (0.1% formic acid), and mobile phase B was acetonitrile. The elution gradient was set to 0% B, 0 – 1.0 min; 0 – 40% B, 1.0 – 3.0 min; 40% B, 3.0 – 5.0 min; 40% – 70% B, 5.0 – 5.1 min; 70% B, 5.1 – 7.0 min; 70% – 80% B, 7.0 – 7.1 min; and 0% B, 14.1 – 16.0 min. The flow rate was 0.4 mL/min, the column temperature was 40 ℃, and the injection volume was 5 μL.

Mass spectrometry parameter conditions: ESI source conditions were as follows: capillary voltage 3 – 3.30 kV, sampling cone 40, shock source offset 80, source temperature 100 ℃, desolventizing temperature 250 – 300 ℃, cone gas 50 L/H, desolventizing gas flow rate 59,850 L/H, positive ion scan m/z range 50 – 1200 Da, and negative ion scan m/z range 50 – 1200 Da.

KEGG enrichment analysis of polyphenol metabolites

The identified polyphenols were submitted to KEGG (http://www.genome.jp/Kegg/) for pathway enrichment analysis.

Laser confocal microscopy analysis

In brief, 6-mm diameter blocks of *A. alternata* and *Alternaria* spp. were inoculated on the drug-containing plate (90 mm) and cultured at 28 ℃ for 5–6 days. Mycelia were collected and stained in SYTOX-Green with a final concentration of 1 μmol/L for 10 min in the dark. The mycelia were washed three times with HBSS buffer. The coverslip was fixed with mounting media, and the slide was immediately observed under a laser confocal microscope.

Determination of cell membrane conductivity

The hyphae required for determination of cell membrane conductivity were grown using the method of Jing et al. (2018) with slight modifications. Thirty blocks of *A. alternata* and *Alternaria* spp. were placed in 300 mL of PDB liquid medium by punching method and cultured in an incubator at 28 ℃ for 5 days to obtain hyphae. The four layers of gauze were arranged on the Buchner funnel, the culture solution on the mycelia was drained under aseptic conditions, and the mycelia were washed with sterile water three times. About 1 g (wet weight) of the mycelium/part was collected and transferred to a beaker containing sterile distilled water. The fermentation broth was added to a final volume concentration of 10%, and sterile distilled water was used as blank control. Conductivity was measured at room temperature from 0 to 17 h and recorded as S1 for the experimental group and as S0 for the blank control group. The treatment was repeated three times. Each experimental group and the blank control group were heated in a boiling water bath for 10 min. The samples were cooled to 25 ℃ with tap water, and final conductivity was measured and recorded as S2. According to the above-measured values, relative conductivity could be calculated using the formula $\frac{S1-S0}{S2-S0}$ (Ai et al. 2023).

Statistical analysis

All samples were subjected to three parallel experiments, and six biological replicates were performed in the metabolomics analysis. Office Excel 2019 was used to calculate mean, standard deviation, and other related parameters. Bar and line graphs were prepared using Origin 2018. SPSS 26 was used to analyze the experimental data for significance and regressions. The metabolome raw and final data were formatted using Analysis Base File Converter software and compared with the metabolite public database (http://prime.psc.riken.jp/compms/msdial/main.html#MSP) using MS-DIAL 4.80 software. Principal component analysis (PCA) and cluster heat mapping were carried out using R Studio. Orthogonal partial least-squares discrimination analysis (OPLS-DA) and OPLS-DA model validation were conducted on SIMCA 14.1.

Results

Inhibition of fungal activity of two plant pathogenic fungi by different ratios of fermented waste water from agar processing industries

After mixed fermentation of the waste water and LB medium in different proportions, the percentage of fermented waste water in the 25% experimental group showed a significant increase in the inhibition rate of *A. alternata* and *Alternaria* spp.; both of which were better than the positive control group and reached the highest rate of 99.9% and 96.1%, respectively (Fig. 1).

MIC of fermented crude extract against *A. alternata* and *Alternaria* spp.

MIC is the minimum drug concentration that inhibits the growth of microorganisms (Cen et al. 2021). After the fermentation of waste water from agar processing industries, the metabolites produced were crudely extracted, and the MIC of the crude extract against *A. alternata* and *Alternaria* spp. both was 0.156 μg/mL (Table 1). After *B. subtilis* fermented the waste water, the metabolites produced had an inhibitory effect on the two plant pathogenic fungi.

Polyphenol metabolite analysis

Analysis of the metabolic characteristics of waste water from agar processing industries before and after fermentation with *B. subtilis*

The main components of waste water were shown in (Table. S1). The main components of waste water from agar processing were polysaccharides such as cellulose, proteins such as phycobiliproteins, polyphenols such as anthocyanins, fats such as grease, and inorganic elements such as N and P. Seaweed contains polyphenol substances, which are the main active antifungal components (Zhao et al. 2022). During the fermentation process, phenolic compounds could be converted into unique metabolites by the methylation, carboxylation, sulfate conjugation, hydroxylation, and oxidation capabilities of microorganisms (Gulsunoglu-Konuskan and Kilic-Akyilmaz 2022). Therefore, polyphenols were selected as the main target metabolites for analysis. The

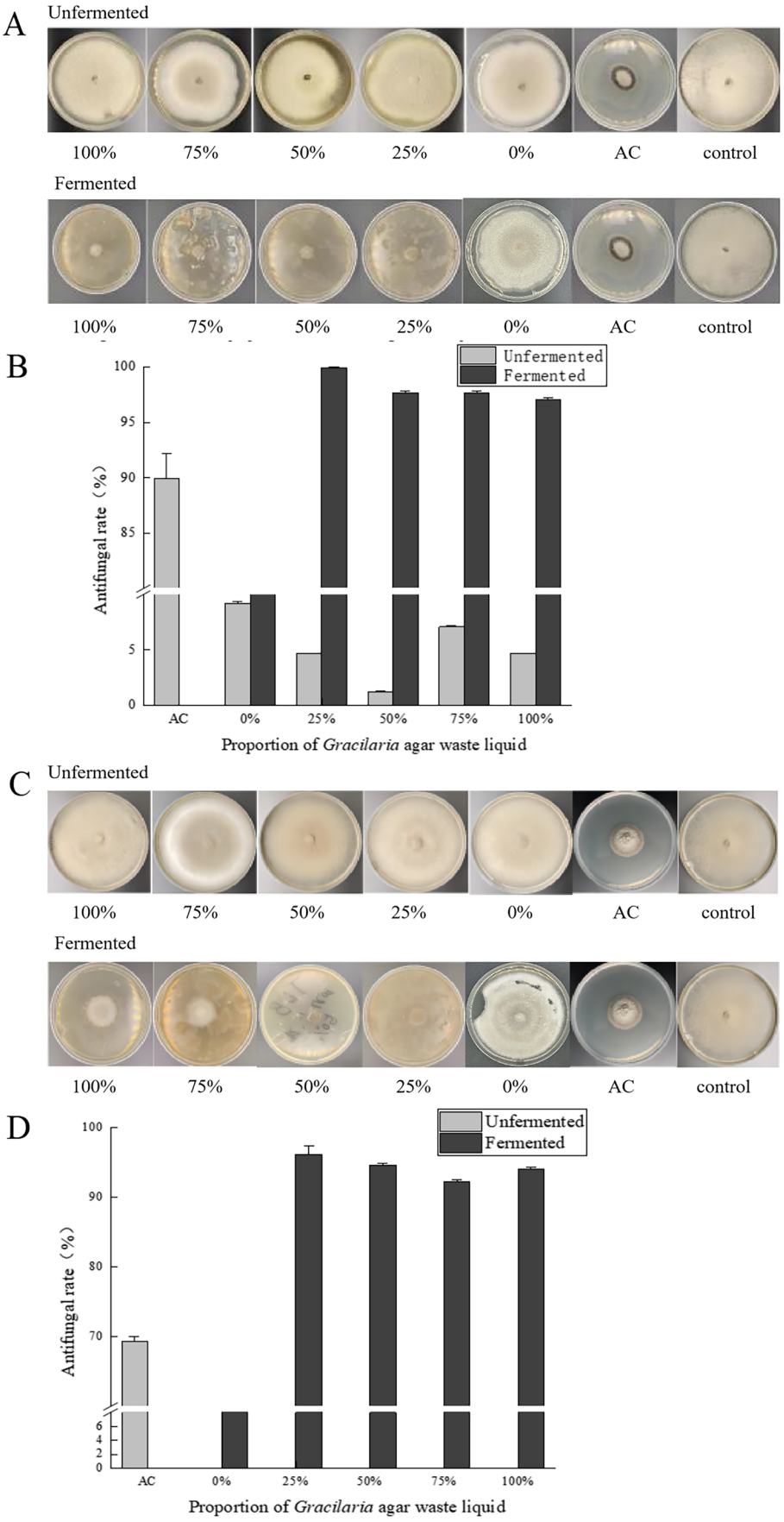

Fig. 1 Antifungal plate and antifungal rate of waste water on *Alternaria alternata* and *Alternaria* spp. after fermentation. **A, B** antifungal plate and antifungal rate against *Alternaria alternata*; **C, D** antifungal plate and antifungal rate against *Alternaria* spp. Note: AC: positive control; 0%, 25%, 50%, 75%, and 100% were the percentages of waste water in the medium, respectively

Table 1 MIC of fermented crude extract against two plant pathogenic fungi

Final concentration/ ($\mu g \cdot mL^{-1}$)	Antifungal rate (%)	
	Alternaria alternata	*Alternaria* spp.
2.500	37.24 ± 0.81	19.24 ± 1.75
1.250	43.31 ± 2.03	14.73 ± 2.24
0.625	38.87 ± 4.46	8.04 ± 2.23
0.313	16.59 ± 2.03	4.47 ± 2.13
0.156	0 ± 0	0 ± 0
0.078	0 ± 0	0 ± 0
0.039	0 ± 0	0 ± 0

reproducibility of the metabolite extraction and detection (i.e., technical duplication) was determined by overlaying the total ion flow diagrams (Fig. S2) (TIC diagrams) obtained from the mass spectrometric detection analysis of different QC samples. The TIC plots of the six QC samples in positive and negative ion modes were highly superimposed, indicating good stability of the instrument and good reproducibility of metabolite detection for the same sample at different time points, thereby ensuring the reproducibility and reliability of the data.

Cluster analysis and PCA of metabolites of waste water from agar processing industries before and after fermentation with *B. subtilis*

Qualitative and relative quantitative information on metabolites was subjected to cluster heat map analysis and PCA to observe changes in polyphenolic compounds in waste water from agar processing industries under *B. subtilis* fermentation. The hierarchical clustering heat map analysis divided all samples into two main clusters based on the accumulation of polyphenolic metabolites in different samples, with cluster 1 being K1B and cluster 2 being K0B. The hierarchical relationships in the cluster heat map indicated that the polyphenolic metabolite profile of waste water fermented by *B. subtilis* was significantly different from that of the unfermented control (Fig. 2). The relative contents of dicoumarolum, wulignan A1, glycitin, procyanidin A1, acetamidocumarin, tiliroside, and velutin significantly increased in the fermentation optimum group. Group differences in the samples were verified by PCA (Fig. 3). The PCA results revealed two principal components that best interpreted the raw multidimensional data; different colored scatters represent different mixing ratios between the waste water and the medium, and different shapes represent the fermented and unfermented samples. The first principal component (PC1) and the second principal component (PC2) correspond to the horizontal and vertical coordinates of the graph, respectively, and they explained 46.4% and 22.8% of the total variance, respectively. The fermented and unfermented sample fractions were separated by PC1 mainly in two regions around the zero scale line, indicating that fermentation could effectively alter the polyphenolic profile of the waste water.

Analysis of OPLS-DA and screening of differential metabolites before and after fermentation of waste water from agar processing industries by *B. subtilis*

In the score chart between K0B and K1B, the horizontal coordinates indicated the predicted principal components, which showed the differences between the groups after fermentation; the vertical coordinates indicated the orthogonal principal components, which showed the differences within the groups; and the percentage indicated the degree to which the component explains the data set (Fig. 4A). Each point represented a sample, and the same group of the samples was represented by one color. The horizontal coordinates showed that K0B and K1B were clearly distinguished on either side of $x = 0$, indicating significant differences in the polyphenol metabolites in waste water from agar processing industries fermented by *B. subtilis* as well as between groups. Fermentation greatly changed the components of the waste liquid, providing various possibilities for fungal inhibition. The OPLS-DA model was further tested with 200 permutations to evaluate its accuracy and obtain accurate differential metabolites for subsequent analyses. The optimal group had Q^2 greater than 0.5 after *B. subtilis* fermentation versus unfermented ($R^2X = 0.67$, $R^2Y = 0.993$, $Q^2 = 0.978$), indicating that the OPLS-DA model could be a good predictor for subsequent screening of differential metabolites (Fig. 4B).

Based on the OPLS-DA results, the variable importance in the projection (VIP) of the OPLS-DA model for multivariate analysis and the *P* value obtained by the *T*-test was obtained. Based on VIP value greater than 1 and *P* value less than 0.05, the FC value of "-" or greater than 1.5 was judged as upregulated metabolic differential; the FC value of 0 or less than 0.5 was judged as downregulated metabolic differential. Forty-eight differential metabolites were found between K0B and K1B (16 upregulated and 32 downregulated). The upregulated metabolites are glycycoumarin, glycitin, procyanidin A1, coniferyl aldehyde, and velutin (Table 2).

Metabolic pathway analysis of polyphenols

The identified metabolites were located and annotated by KEGG on the metabolic pathways. This method not only provides all possible metabolic pathways but also comprehensively indicates the enzymes that catalyze each step of the reaction (Kanehisa 2017). Polyphenol metabolites were submitted to KEGG for pathway enrichment analysis. During

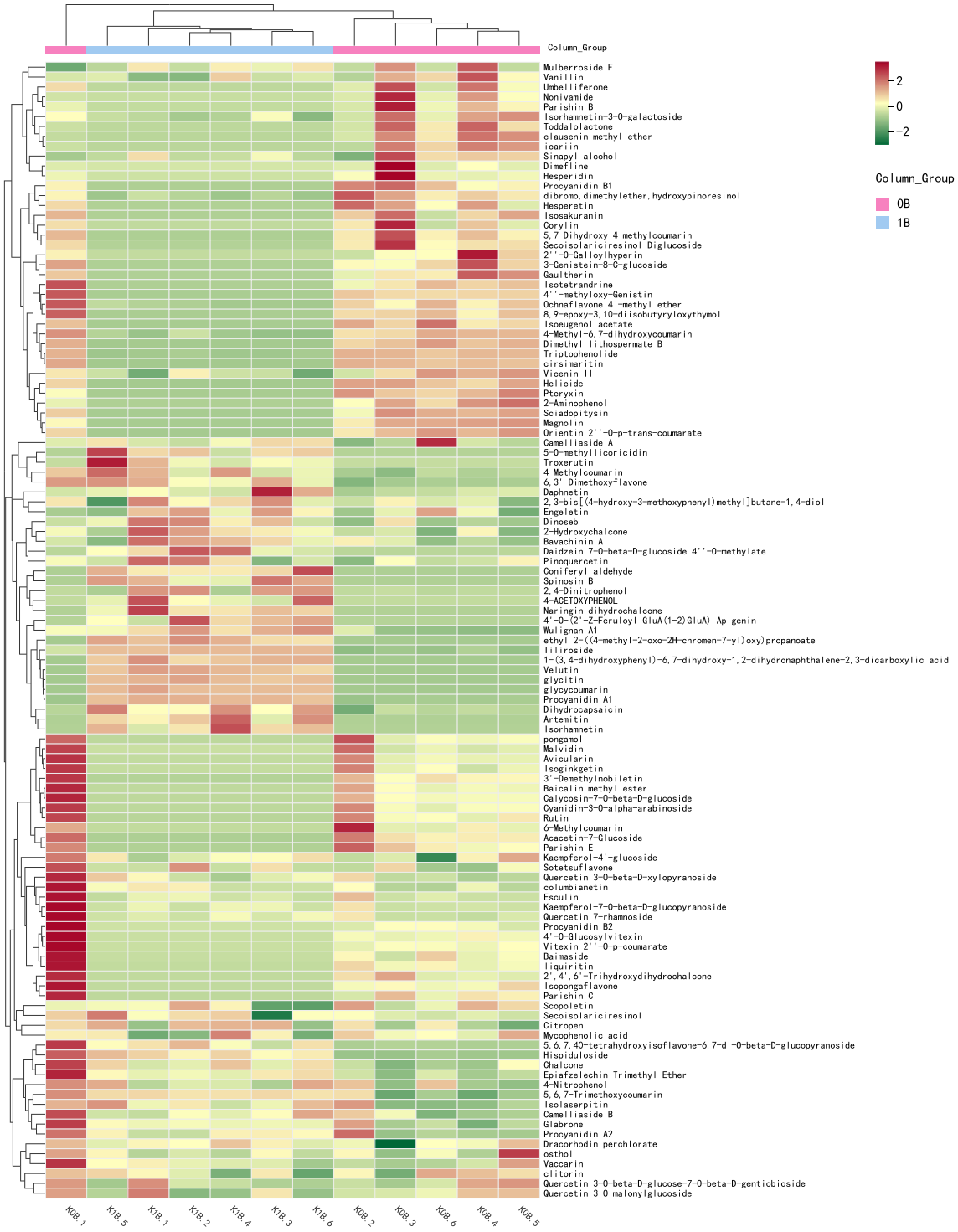

Fig. 2 Cluster heat map of polyphenols detected in waste water before and after fermented of *Bacillus subtilis*. Note: K0B.1-K0B.6: waste water unfermented group; K1B.1-K1B.6: waste water fermented group

fermentation, metabolites were involved in five metabolic pathways, including isoflavonoid biosynthesis, biosynthesis of phenylpropanoids, phenylpropanoid biosynthesis, tryptophan metabolism, and flavonoid biosynthesis pathways. The key secondary metabolites in these pathways were phenols, flavonoids, flavones, coumarins, and phenylpropanoids, whose contents significantly changed after fermentation. Among the detected polyphenol metabolites, the contents

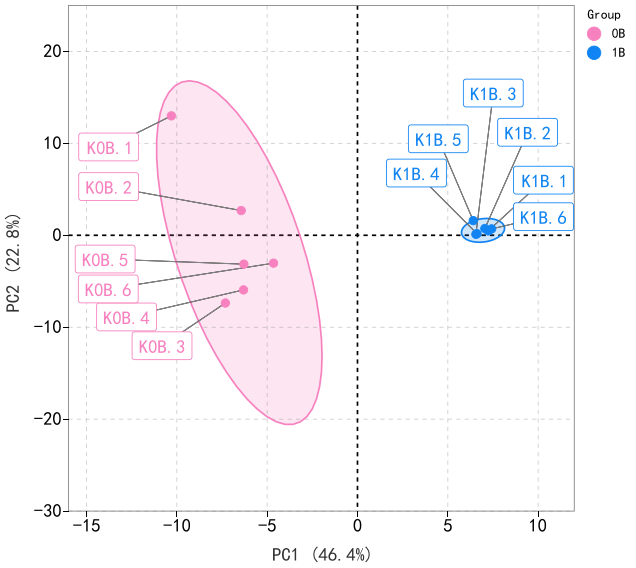

Fig. 3 PCA of polyphenols detected in waste water before and after fermented of *Bacillus subtilis*. Note: K0B.1-K0B.6: waste water unfermented group; K1B.1-K1B.6: 25% waste water fermented group

of glycitin and coniferyl aldehyde increased substantially after fermentation. Glycitin was produced by isoflavonoid biosynthesis pathway from liquiritigenin (Fig. 5). Coniferyl aldehyde was produced by phenylpropanoid biosynthesis pathway from L-phenylalanine and L-tyrosine (Fig. 5). In addition, the differential metabolites 2-aminophenol, hesperetin, and umbelliferone were downregulated after fermentation. These metabolites involved in competitive pathways (such as biosynthesis of phenylpropanoids and flavonoids biosynthesis) were weakened, promoting the upregulation of the synthetic active polyphenol pathway, such as isoflavonoid biosynthesis and phenylpropanoids biosynthesis (Fig. 5). The metabolic pathways of *B. subtilis* to synthesize antifungal active substances glycitin and coniferyl aldehyde were enhanced.

Laser confocal fluorescence microscopy observation

SYTOX Green (SG) fluorescent nucleic acid staining dye was used in this study; it penetrates into fungal cells and binds to nucleic acids when the plasma membrane integrity

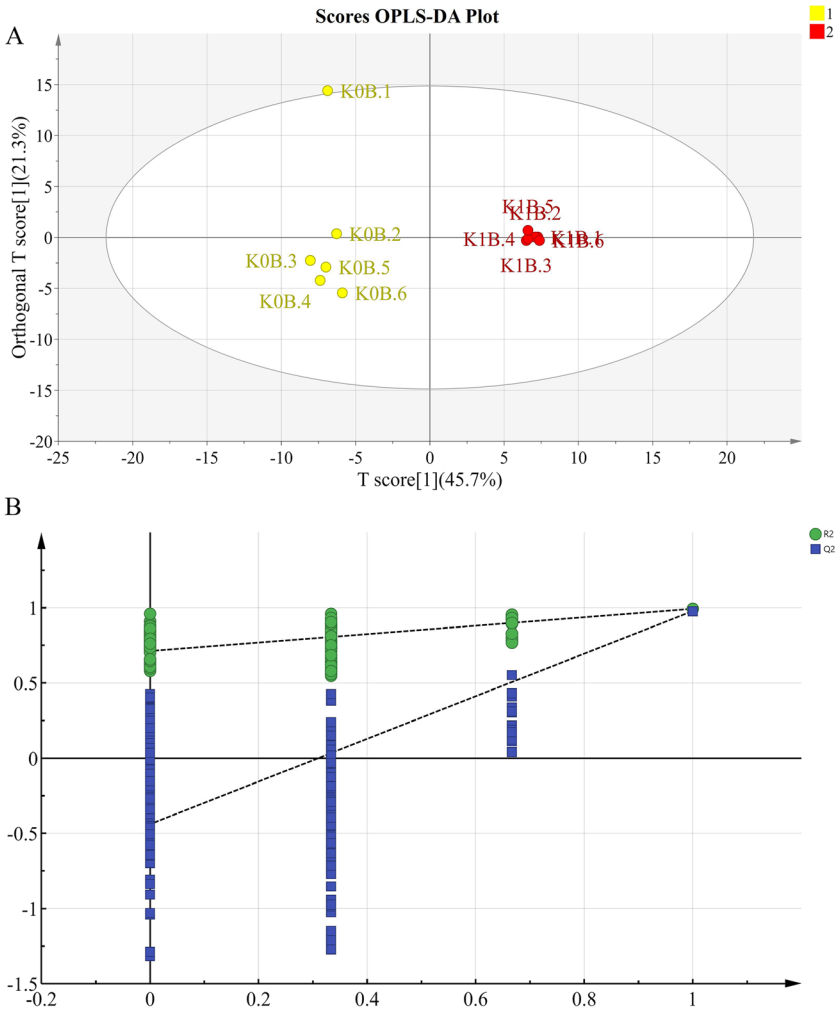

Fig. 4 OPLS-DA score and model validation plot. Note: K0B.1-K0B.6: 25% waste water unfermented group; K1B.1-K1B.6: 25% waste water fermented group

Table 2 Differential metabolites of K0B and K1B

Metabolite name	VIP	*P* value	Fold change	Type
Glycycoumarin	1.47	0.00	—	Up
Glycitin	1.47	0.00	—	Up
Procyanidin A1	1.47	0.00	5.31	Up
Velutin	1.45	0.00	—	Up
Tiliroside	1.44	0.00	3.68	Up
Ethyl 2-((4-methyl-2-oxo-2H-chromen-7-yl)oxy)propanoate	1.42	0.00	—	Up
Coniferyl aldehyde	1.29	0.00	—	Up
Wulignan A1	1.27	0.00	2.27	Up
Spinosin B	1.25	0.00	—	Up
Artemitin	1.24	0.00	—	Up
Naringin dihydrochalcone	1.23	0.01	—	Up
Dihydrocapsaicin	1.21	0.00	1.72	Up
Isorhamnetin	1.20	0.01	—	Up
4′-O-(2′-Z-Feruloyl GluA(1–2)GluA) apigenin	1.16	0.01	—	Up
5-O-methyllicoricidin	1.16	0.01	—	Up
Daidzein 7-O-beta-D-glucoside 4"-O-methylate	1.05	0.02	—	Up
Triptophenolide	1.47	0.00	0.29	Down
Cirsimaritin	1.47	0.00	0.00	Down
Dimethyl lithospermate B	1.45	0.00	0.23	Down
Helicide	1.44	0.00	0.00	Down
Orientin 2″-O-p-trans-coumarate	1.42	0.00	0.00	Down
4-Methyl-6,7-dihydroxycoumarin	1.41	0.00	0.13	Down
Sciadopitysin	1.40	0.00	0.00	Down
Magnolin	1.40	0.00	0.00	Down
Pteryxin	1.37	0.00	0.00	Down
Isoeugenol acetate	1.35	0.00	0.00	Down
4″-Methyloxy-genistin	1.34	0.00	0.00	Down
8,9-Epoxy-3,10-diisobutyryloxythymol	1.34	0.00	0.00	Down
5,7-Dihydroxy-4-methylcoumarin	1.33	0.00	0.00	Down
Isosakuranin	1.30	0.00	0.00	Down
2-Aminophenol	1.29	0.00	0.00	Down
Procyanidin B1	1.28	0.00	0.00	Down
Ochnaflavone 4′-methyl ether	1.27	0.00	0.18	Down
Acacetin-7-glucoside	1.27	0.00	0.00	Down
Isotetrandrine	1.27	0.00	0.00	Down
Gaultherin	1.27	0.00	0.00	Down
3-Genistein-8-C-glucoside	1.26	0.00	0.00	Down
Hesperetin	1.25	0.00	0.00	Down
Secoisolariciresinol diglucoside	1.24	0.01	0.00	Down
Parishin E	1.22	0.00	0.00	Down
3′-Demethylnobiletin	1.15	0.01	0.00	Down
Clausenin methyl ether	1.11	0.02	0.00	Down
Icariin	1.10	0.02	0.00	Down
Umbelliferone	1.07	0.03	0.00	Down
Toddalolactone	1.06	0.03	0.00	Down
Rutin	1.06	0.02	0.00	Down
Parishin C	1.03	0.03	0.00	Down
Corylin	1.01	0.05	0.00	Down

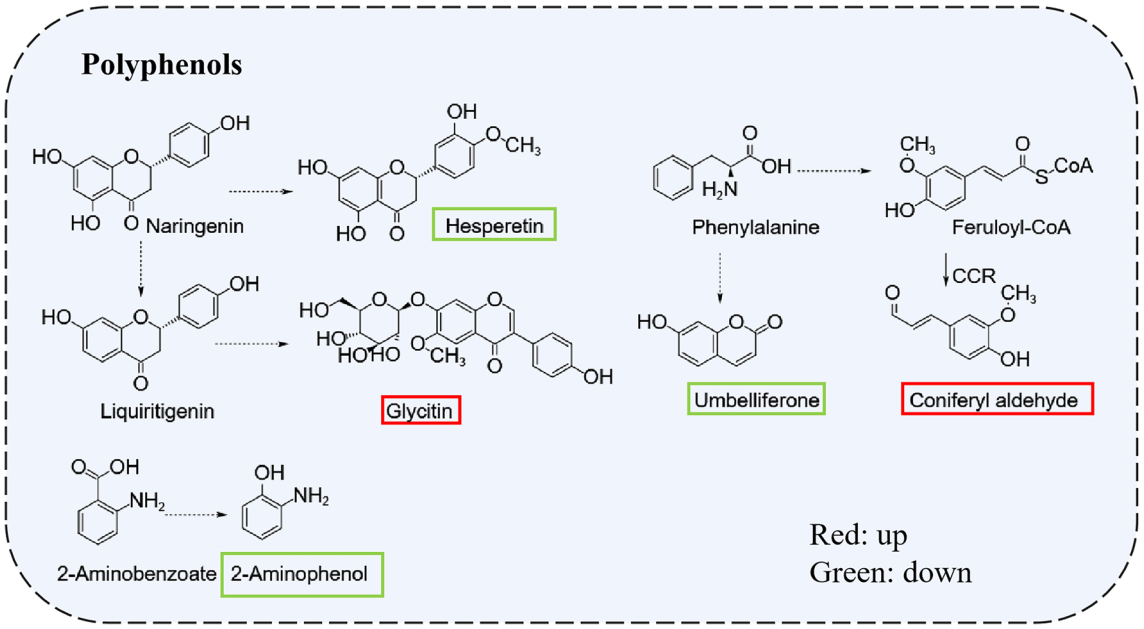

Fig. 5 Metabolic pathway of polyphenols

of the fungus was compromised (Machado and Soares 2012). After the two plant pathogenic fungi were treated with 25% (v/v) fermentation supernatant, laser confocal microscopy images and corresponding brightfield images were taken up by hyphal SG (Fig. 6; scale bar 25 μm). Under confocal conditions, the blank group did not fluoresce, and the positive control group and the experimental group fluoresced. The fluorescence intensity of the experimental group was stronger than that of the positive control group, indicating that the SG-labeled nucleic acids of pathogenic fungal hyphae treated with fermented supernatant had enhanced plasma membrane permeability.

Determination of the effect of fermentation broth on the permeability of mycelial cell membrane by conductivity method

The permeability of the mycelium cell membrane was measured by electric conductivity test. The change trend of the electrical conductivity of each experimental group with increasing treatment time of *A. alternata* was shown in Fig. 7A. The conductivity of each experimental group had no obvious change trend at 0 – 6 h, indicating the existence of the mycelial cell wall of the active component. At 7 – 15 h, the conductivity of 25% mycelia in the optimal group showed an upward trend, indicating that the mycelium was destroyed. This phenomenon resulted in the dissolution of intracellular ions, leading to increases in ion concentration, conductivity, cell permeability, dissolved substances, cell death rate, and antifungal effect. The mycelial conductivity of 25% optimal group tended to be flat at 15 – 17 h, while the other groups showed a downward trend at 13 – 17 h, which might be due to the combination of dissolved ions and components in the sample to reduce the ion concentration and decrease the conductivity. The change trend of electrical conductivity of each experimental group with increasing treatment time of *Alternaria* spp. was shown in Fig. 7B. The trend of hyphal conductivity in the optimal group was basically the same as that in the optimal group of *A. alternata.* The conductivity of the other groups fluctuated significantly from 7 to 17 h and finally showed a downward trend. The dissolved ions might combine with the components in the sample, reducing the ion concentration and conductivity.

Discussion

The results of recent studies on inhibiting *Alternaria* growth and increasing antifungal activity through *B. subtilis* fermentation were summarized in (Table. S2). According to Harish et al., different *B. subtilis* strains and antifungal lipopeptides were extracted and identified by HPLC, and the antifungal activities of lipopeptides from *B. subtilis* were evaluated. The results showed that strain T6 had the highest antifungal activity against *A. alternata* (85.88%) (Harish et al. 2023). Zhang et al. reported that after treating *Alternaria solani* with *B. subtilis* ZD01 fermentation broth under greenhouse conditions, the spore germination rate of *Alternaria solani* was 16.67%, which

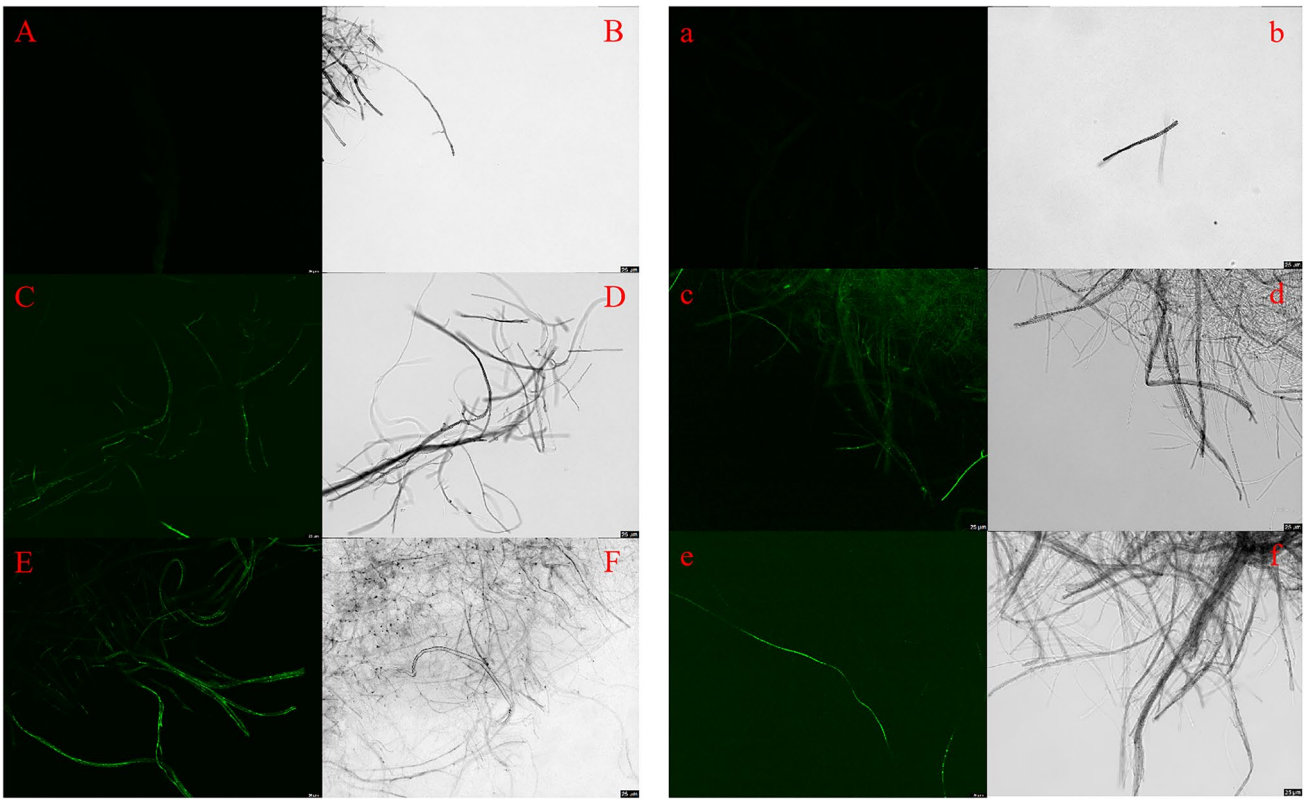

Fig. 6 Laser confocal image of two pathogenic fungi treated with fermentation crude extract by SYTOX-Green staining. **A–F** *Alternaria alternata*; **a–f** *Alternaria* spp. Note: **A, C, E, a, c, e** were SG fluorescence observed by confocal laser microscopy; **B, D, F, b, d, f** were bright field image; **A, B, a, b** were blank control; **C, D, c, d** were positive control; **E, F, e, f** were experimental groups

was 75% lower than the blank group (Zhang et al. 2022). Li et al. reported that *Bacillus velezensis* HY19 fermentation broth significantly inhibited the growth of gray mold in tomato, with inhibition rates of 47.99%, 60.54%, 92.5%, and 99.6% at 0.0125%, 0.025%, 0.05%, and 0.1% concentrations of fermentation crude extracts, respectively (Li et al. 2022b). Dikbaş et al. partially purified *Lactobacillus coryniformis* 3N11 chitinase and measured its antifungal activity against *A. alternata* ET57 in an in vitro experiment. The results showed that the chitinase obtained from *Lactobacillus coryniformis* 3N11 had an inhibitory rate of 20.83 to 54.17% against *A. alternata* at different doses (Dikbaş et al. 2022). Kim et al. isolated a plant growth-promoting bacterium, *B. subtilis* SA-15, was isolated from non-agricultural soil. In field experiments, its therapeutic effect on the large spot disease caused by *Zoysia japonica Rhizoctonia solani* AG 2–2 (IV) was 51.2–92.0% (Kim et al. 2021). Compared with the results of previous research, the antifungal effect of this study was excellent, and the group fermented with 25% waste water from agar processing industries as the best group. The inhibition rates against *A. alternata* and *Alternaria* spp. were as high as 99.9% and 96.1%, respectively. This might be related to the upregulation of polyphenol components during the fermentation process of *B. subtilis*. So *B. subtilis* fermentation of seaweed waste water showed excellent antifungal function.

Zhao et al. isolated a novel polyphenol derivative from the root bark of *Periploca sepium* and found that it significantly inhibited the growth of *Alternaria*, with a MIC of 3.13 μg/mL (Zhao et al. 2019). Deng et al. reported the inhibitory effect of different solvent extracts of *Oudemansiella mucida* fermentation broth on five plant pathogens. The MIC of the ethyl acetate extract of fermented broth against *A. alternata* was 5 mg/mL, which was higher than the 0.156 μg/mL of the present results (Deng et al. 2020). It was further indicated the high antifungal activity of the crude extract from the fermentation of waste water from agar processing industries fermented by *B. subtilis*.

A total of 115 polyphenolic flavonoids were compared by UPLC-Q-TOF–MS analysis. The results of the clustering heat map showed that the profile of polyphenol metabolites of the waste water from agar processing industries fermented by *B. subtilis* was significantly different from that of the unfermented control group. Munir et al. used LC–ESI–MS/MS to compare the metabolic profiles of citrus plants before and after treatment with endophytic *B. subtilis* L1-21; the highest percentages of organic acids, flavone, amino acid

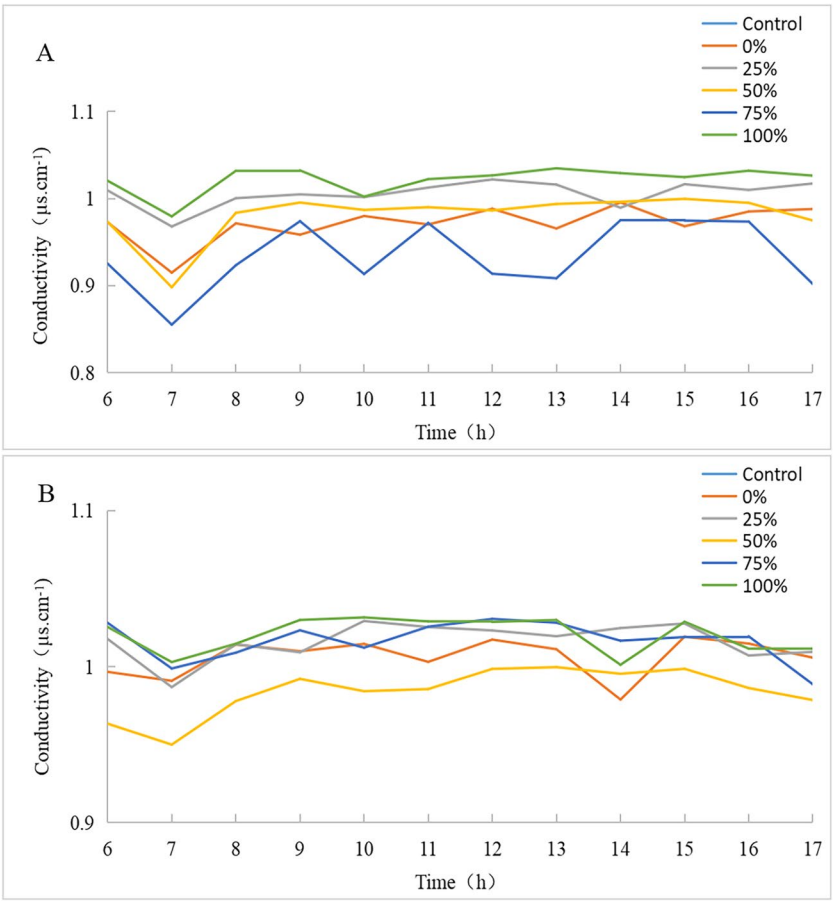

Fig. 7 Effects of treatment of waste water fermentation crude extract on conductivity of two pathogenic fungi. **A** *Alternaria alternata*; **B** *Alternaria* spp

derivatives, flavone C-glycosides, nucleotide derivatives, and flavonol were effective in inhibiting the growth of citrus ulcer fungus (Munir et al. 2020). It was further proved that the fermentation of *B. subtilis* could significantly change the metabolic profile of the fermentation broth, increase the content of polyphenolic flavonoids, and thus inhibit the growth of plant pathogens.

Based on OPLS-DA, 48 differential metabolites were screened, among which the contents of flavonoid polyphenols such as glycycoumarin, glycitin, procyanidin A1, coniferyl aldehyde, and velutin were increased. By comparing the growth of alfalfa before and after *B. subtilis BS* TTL1 treatment, Li et al. reported that inter-root soil metabolite regulation (e.g., upregulated of amino acids, flavonoids, fatty acids, and carbohydrates) promoted the growth of alfalfa and the mitigation of heavy metal toxicity in the presence of *B. subtilis* (Li et al. 2021b). Hu et al. used a mixture of *Lactiplantibacillus plantarum* B7 and *B. subtilis natto* to ferment rose residue and compared the metabolites before and after fermentation by LC–MS/MS. The results showed that the expression of coumaric acid, gallic acid, quercetin, naringenin, and kaempferol was upregulated, and their upregulation was responsible for their high antioxidant and antifungal capacities (Hu et al. 2022). Our data (Table 2) also showed that the contents of polyphenols such as glycitin, velutin, and coniferyl aldehyde were upregulated after fermentation. Therefore, these upregulated flavonoid polyphenols that were speculated might be the material basis for potentially enhancing the inhibitory activity against the two pathogenic fungi tested. In future research, specific types of polyphenols would be further selected to confirm their antifungal activity to verify this speculation.

In this study, based on the KEGG analysis, isoflavonoid biosynthesis, biosynthesis of phenylpropanoids, phenylpropanoid biosynthesis, tryptophan metabolism, and flavonoid biosynthesis pathways were enriched, which were associated with five specific metabolites. The relevant descriptions of the pathways are listed in Table S3. During the fermentation process of waste water from agar processing industries by *B. subtilis*, the macromolecular sugars contained in the waste water would be consumed through glycolysis. It was then converted into polyphenols through the phenylpropanoid biosynthesis and isoflavonoid biosynthesis pathways. At the same time, the weakening of some competitive pathways (such as biosynthesis of phenylpropanoids and flavonoid biosynthesis) also promotes the production of polyphenols. Relevant references also showed that bacteria could produce polyphenols. Marchut-Mikołajczyk et al.

isolated three strains of endophytic bacteria from common stinging nettle and found that each of the isolated bacterial strains was capable of producing biosurfactants and polyphenols (Marchut-Mikołajczyk et al. 2023). Sarjono et al. found that isolates of endophytic bacteria that symbiotes with the papaya leaves were able to produce alkaloid, flavonoids, saponins, tannins, and triterpenoids compounds that act as antioxidant and antibacterial (Sarjono et al. 2019). The results showed that the original substances in waste water from agar processing industries were consumed after fermentation by *B. subtilis* and converted into polyphenols through the phenylpropanoid biosynthesis and isoflavonoid biosynthesis pathways.

Previous studies have shown that the upregulated differential metabolites in corn treated by *B. subtilis* were mainly involved in flavonoid biosynthesis and flavone and flavonol biosynthesis pathways (Shao et al. 2023). Mashabela et al. reported that the metabolites in the rhizosphere and leaves of *Triticum aestivum L.* were changed before and after treatment with *B. subtilis*; alterations in these metabolites affected important pathways facilitating the plant's primary and secondary metabolism, including phenylalanine, tryptophan biosynthesis, phenylpropanoid biosynthesis, and phenylalanine metabolism (Mashabela et al. 2022). Gao et al. found that during the fermentation of soy milk by *B. subtilis* BSNK-5, macromolecular substances were degraded into small molecular substances through pathways such as amino acid and lipid metabolism, thus affecting the nutritional and functional properties of fermented soy milk (Gao et al. 2022). This was consistent with the metabolic pathways involved in secondary metabolites of *B. subtilis* in this study, indicating that *B. subtilis* does have the ability to generate these pathways (such as phenylpropanoid biosynthesis and isoflavonoid biosynthesis). And *B. subtilis* could synthesize polyphenols through these pathways.

Tian et al. conducted staining by fluorescent SYTO 9 and propidium iodide (PI) and observed the samples under laser confocal microscope; after treatment with thymol, the green fluorescence was significantly reduced and the red fluorescence was significantly increased, indicating that thymol-induced damages to the cell membrane of *E. sakazakii* and inhibited cell growth (Tian et al. 2020). Shreaz et al. showed that the cell membrane of *Candida* was destroyed by coniferaldehyde, causing cell surface damage and wrinkled as well as leakage of cell contents (Shreaz et al. 2013). Alshaibani et al. reported that cranberry proanthocyanidins increased the membrane permeability and inhibited microbial growth by weakening the composition of the outer membrane of diarrheagenic *Escherichia coli* and causing perforation (Alshaibani et al. 2017). Relevant references showed that conifer aldehyde and proanthocyanidins could damage cell structures. In this study, polyphenols such as coniferaldehyde and procyanidin A1 also showed upregulation after fermentation. This indicated that polyphenols might be the material basis for destroying the cell structure of the two plant pathogenic fungi.

Electrical conductivity is an important indicator of cell membrane permeability, and a larger value indicates more leakage of electrolytes and more damage to the cell membrane. (Yuan et al. 2023a). The cell conductivity analyses of *A. alternata* and *Alternaria* spp. showed that the cell membrane of fungi treated with fermentation broth was destroyed, resulting in the dissolution of intracellular ions, increased conductivity, and fungal cell death, thereby achieving antifungal effect. Duan et al. studied the effect of H_2S on the membrane permeability of *Botryosphaeria dothidea* cells and reported that the extracellular conductivity was significantly increased after H_2S treatment (Duan et al. 2022). Yuan et al. reported that combined SAEW + UV treatment significantly increased the cell membrane conductivity of *Salmonella enteritidis* (Yuan et al. 2023b), consistent with the results of the present study. Overall, the upregulation of coniferyl aldehyde and procyanidin A1 might be the reason why the fermentation broth destroys the fungal cells, leading to increases in extracellular conductivity and plasma membrane permeability.

In summary, the results of this study showed that the fermentation of *B. subtilis* could effectively transform into polyphenol antifungal substances and improve the antifungal activity of the fermentation supernatant against *A. alternata* and *Alternaria* spp. The MIC against two plant pathogenic fungi was 0.156 μg/mL. Metabolomics analysis showed that the upregulation of flavonoid polyphenols such as coniferyl aldehyde, glycycoumarin, glycitin, and procyanidin A1 might be the material basis for the potential enhanced inhibitory activity against the two pathogenic fungi. Based on the KEGG enrichment analysis, five metabolic pathways including isoflavonoid biosynthesis, biosynthesis of phenylpropanoids, phenylpropanoid biosynthesis, tryptophan metabolism, and flavonoid biosynthesis were enriched. The laser confocal microscopy and cell conductivity analyses of pathogenic fungi showed that the cell wall and cytoplasm of fungi treated with fermentation broth were destroyed, resulting in the dissolution of intracellular ions, increased conductivity and fungal cell death, thereby achieving antifungal effect. The supernatant of waste water from agar processing industries co-fermented with *B. subtilis* has the potential to develop new natural antifungal agents, which provides a theoretical basis for the synthesis of antifungal agents by microbial fermentation and the resource utilization of seaweed agar waste.

Supplementary Information The online version contains supplementary material available at https://doi.org/10.1007/s00253-023-12891-9.

Author contribution YYW: conceptualization, methodology, formal analysis, and writing—original draft. BYD: methodology. QYL and

YYL: analyzed data. XPD, MJZ, and YBZ: investigation. ZDJ, QBL, and HN: funding acquisition. ZPL and JFC: funding acquisition, writing—review and editing, and supervision. All authors read and approved the manuscript.

Funding This work was funded by the National Natural Science Foundation of China (No. 22038012), the Major Special Topics of Science and Technology of Fujian Province, China (No. 2020NZ012015), the Natural Science Foundation of Fujian Province, China (No. 2019J01700), the Open Foundation of state key Laboratory of Environmental Criteria and Risk Assessment, Chinese Research Academy of Environmental Sciences (No. SKLECRA20160FP06), and the Department of Education Foundation of the Fujian Province (No. JAT200238).

Data availability The authors do not have permission to share data.

Declarations

Ethical approval This article does not contain any studies with human participants or animals performed by any of the authors.

Competing interests The authors declare no competing interests.

References

Admassie M, Woldehawariat Y, Alemu T (2022) In vitro evaluation of extracellular enzyme activity and its biocontrol efficacy of bacterial isolates from pepper plants for the management of *Phytophthora capsici*. Biomed Res Int 2022:6778352

Ai SN, Chen LY, Huang JW, Li Q, Xie YL (2023) Synergistic antifungal effect of citral and eugenol against the growth of *Aspergillus flavus*. J Henan Univ Tech 44(01):59–67

Ali GS, El-Sayed ASA, Patel JS, Green KB, Ali M, Brennan M, Norman D (2016) Ex vivo application of secreted metabolites produced by soil-inhabiting *Bacillus* spp. efficiently controls foliar diseases caused by *Alternaria* spp. Appl Environ Microbiol 82(2):478–490

Alshaibani D, Zhang R, Wu VCH (2017) Antibacterial characteristics and activity of *Vaccinium macrocarpon* proanthocyanidins against diarrheagenic *Escherichia coli*. J Funct Foods 39:133–138

Berlanga-Clavero MV, Molina-Santiago C, Caraballo-Rodríguez AM, Petras D, Díaz-Martínez L, Pérez-García A, de Vicente A, Carrión VJ, Dorrestein PC, Romero D (2022) *Bacillus subtilis* biofilm matrix components target seed oil bodies to promote growth and anti-fungal resistance in melon. Nat Microbiol 7(7):1001–1015

Cen QW, Wang ZY, Tang ZX, Zhang Y, Chen T, Xue DW, Xu MF, Bai XL, Zhou T, Shi LE (2021) Initial purification of antimicrobial fermentation metabolites from *Paecilomyces cicadae* and its antimicrobial mechanism. LWT 148:111785

Deng X, Li RS, Zhang YM, Li RR (2020) Preliminary study on antimicrobial activity of fermentation broths of *Oudemansiella mucida*. EES 440(2):022035

Dikbaş N, Uçar S, Tozlu E, Kotan MŞ, Kotan R (2022) Antifungal activity of partially purified bacterial chitinase against *Alternaria alternata*. Erwerbs-Obstbau 65(4):761–766

Duan YN, Chen R, Zhang R, Jiang WT, Chen XS, Yin CM, Mao ZQ (2021) Isolation, identification, and antibacterial mechanisms of *Bacillus amyloliquefaciens* QSB-6 and its effect on plant roots. Front Microbiol 12:746799

Duan B, Du HY, Zhang W, Wang J, Cai ZP, Shen YG, Huang TH, Yuan J, Gan ZY, Chen JY, Zhu LQ (2022) An antifungal role of hydrogen sulfide on *Botryosphaeria dothidea* and amino acid metabolism involved in disease resistance induced in postharvest kiwifruit. Front Plant Sci 13:888647

Gao HY, Li PZ, Xu XX, Zeng Q, Guan WQ (2018) Research on volatile organic compounds from *Bacillus subtilis* CF-3: biocontrol effects on fruit fungal pathogens and dynamic changes during fermentation. Front Microbiol 9:456

Gao YX, Li DF, Tian ZL, Hou LZ, Gao J, Fan B, Wang FZ, Li SY (2022) Metabolomics analysis of soymilk fermented by *Bacillus subtilis* BSNK-5 based on UHPLC-Triple-TOF-MS/MS. LWT 160:113311

Gulsunoglu-Konuskan Z, Kilic-Akyilmaz M (2022) Microbial bioconversion of phenolic compounds in agro-industrial wastes: a review of mechanisms and effective factors. J Agr Food Chem 70(23):6901–6910

Harish BN, Nagesha SN, Ramesh BN, Shyamalamma S, Nagaraj MS, Girish HC, Pradeep C, Shiva Kumar KS, Tharun Kumar KS, Pavan SN, Kavan Kumar V (2023) Molecular characterization and antifungal activity of lipopeptides produced from *Bacillus subtilis* against plant fungal pathogen *Alternaria alternata*. BMC Microbiol 23:179

Hu Y, Wang XY, Qin CQ, Li TT, Liu WH, Ren DF (2022) Fermentation of rose residue by *Lactiplantibacillus plantarum* B7 and *Bacillus subtilis natto* promotes polyphenol content and beneficial bioactivity. J Biosci Bioeng 134(6):501–507

Jing CL, Zhao J, Han XB, Huang RH, Cai DS, Zhang CS (2018) Essential oil of *Syringa oblata* Lindl. as a potential biocontrol agent against tobacco brown spot caused by *Alternaria alternata*. Crop Prot 104:41–46

Kanehisa M (2017) Enzyme annotation and metabolic reconstruction using KEGG. Methods Mol Biol 1611:135–145

Kim YS, Lee KS, Kim HG, Lee GJ (2021) Biocontrol of large patch disease in zoysiagrass (*Zoysia japonica*) by *Bacillus subtilis* SA-15: identification of active compounds and synergism with a fungicide. Horticulturae 8(1):34

Li WZ, Long YH, Mo FX, Shu R, Yin XH, Wu XM, Zhang RQ, Zhang ZZ, He LN, Chen TT, Chen J (2021a) Antifungal activity and biocontrol mechanism of *Fusicolla violacea* J-1 against soft rot in kiwifruit caused by *Alternaria alternata*. J Fungi 7(11):937

Li Q, Xing YN, Fu XW, Ji L, Li TY, Wang JN, Chen GH, Qi ZC, Zhang Q (2021b) Biochemical mechanisms of rhizospheric *Bacillus subtilis*-facilitated phytoextraction by alfalfa under cadmium stress-microbial diversity and metabolomics analyses. Ecotoxicol and Environ Saf 212:112016

Li YM, Xia MY, He PB, Yang QM, Wu YX, He PF, Ahmed A, Li XS, Wang YH, Munir S, He YQ (2022a) Developing *Penicillium digitatum* management strategies on post-harvest citrus fruits with metabolic components and colonization of *Bacillus subtilis* L1–21. J Fungi 8(1):80

Li SP, Xiao QL, Yang HJ, Huang JG, Li Y (2022b) Characterization of a new *Bacillus velezensis* as a powerful biocontrol agent against tomato gray mold. Pest Biochem Physiol 187:105199

Lin P, Yuan HB, Du JK, Liu KQ, Liu HL, Wang TF (2020) Progress in research and application development of surface display technology using *Bacillus subtilis* spores. Appl Microbiol Biot 104(6):2319–2331

Ma X, Wang XB, Cheng J, Nie X, Yu XX, Zhao YT, Wang W (2015) Microencapsulation of *Bacillus subtilis* B99–2 and its biocontrol efficiency against *Rhizoctonia solani* in tomato. Biol Control 90:34–41

Machado MD, Soares EV (2012) Development of a short-term assay based on the evaluation of the plasma membrane integrity of the alga *Pseudokirchneriella subcapitata*. Appl Microbiol Biotechnol 95(4):1035–1042

Marchut-Mikołajczyk O, Chlebicz M, Kawecka M, Michalak A, Prucnal F, Nielipinski M, Filipek J, Jankowska M, Perek Z, Drożdżyński P, Rutkowska N, Otlewska A (2023) Endophytic

bacteria isolated from *Urtica dioica* L.- preliminary screening for enzyme and polyphenols production. Microb Cell Fact 22:169

Mashabela MD, Tugizimana F, Steenkamp PA, Piater LA, Dubery IA, Mhlongo MI (2022) Untargeted metabolite profiling to elucidate rhizosphere and leaf metabolome changes of wheat cultivars (*Triticum aestivum L.*) treated with the plant growth-promoting rhizobacteria *Paenibacillus alvei* (T22) and *Bacillus subtilis*. Front Microbiol 13:971836

Mi TT, Luo DL, Li JK, Qu GF, Sun YZ, Cao S (2023) Carvacrol exhibits direct antifungal activity against stem-end rot disease and induces disease resistance to stem-end rot disease in kiwifruit. Physiol Mol Plant P 127:102065

Munir S, Li YM, He PF, He PB, Ahmed A, Wu YX, He YQ (2020) Unraveling the metabolite signature of citrus showing defense response towards *Candidatus* Liberibacter asiaticus after application of endophyte *Bacillus subtilis* L1–21. Microbiol Res 234:126425

Sarjono PR, Putri LD, Budiarti CE, Mulyani NS, Ngadiwiyana, Ismiyarto, Kusrini D, Prasetya NBA (2019) Antioxidant and antibacterial activities of secondary metabolite endophytic bacteria from papaya leaf (*Carica papaya L.*). IOP Conf Ser: Mater Sci Eng 509:012112

Shao MW, Chen YH, Gong QY, Miao S, Li CJ, Sun YH, Qin D, Guo XJ, Yan X, Cheng P, Yu GH (2023) Biocontrol endophytes *Bacillus subtilis* R31 influence the quality, transcriptome and metabolome of sweet corn. PeerJ 11:e14967

Shreaz S, Bhatia R, Khan N, Muralidhar S, Manzoor N, Khan LA (2013) Influences of cinnamic aldehydes on H^+ extrusion activity and ultrastructure of *Candida*. J Med Microbiol 62:232–240

Tian L, Wang XY, Liu RJ, Zhang D, Wang X, Sun RC, Guo WY, Yang SQ, Li H, Gong GL (2020) Antibacterial mechanism of thymol against *Enterobacter sakazakii*. Food Control 123:107716

Wang S, Zhang YJ, Mandlaa SZY, Chen ZJ (2022) Properties and mechanism of the antimicrobial peptide APT produced by *Lactobacillus* ALAC-4. LWT 165:113713

Wang YR, Yang QY, Godana EA, Zhang Y, Zhang HY (2023) Ultrastructural observation and transcriptome analysis provide insights into mechanisms of *Penicillium expansum* invading apple wounds. Food Chem 414:135633

Yuan YH, Liu LX, Guo L, Wang L, Liu YG (2023a) Antibacterial mechanism of rose essential oil against *Pseudomonas putida* isolated from white *Hypsizygus marmoreus* at cellular and metabolic levels. Ind Crop Prod 196:116523

Yuan XY, Li YJ, Mo QN, Zhang BB, Shu DQ, Sun LN, Zhao XH, Zhang R, Zheng JH, Jia YQ, Zang YT (2023b) Antibacterial activity and mechanism of slightly acidic electrolyzed water combined with ultraviolet light against *Salmonella enteritidis*. Food Control 148:109681

Zhang Y, Wu YT, Zheng W, Han XX, Jiang YH, Hu PL, Tang ZX, Shi LE (2017) The antibacterial activity and antibacterial mechanism of a polysaccharide from *Cordyceps cicadae*. J Funct Foods 38:273–279

Zhang D, Qiang R, Zhou ZJ, Pan Y, Yu SQ, Yuan W, Cheng JN, Wang JH, Zhao DM, Zhu JH, Yang ZH (2022) Biocontrol and action mechanism of *Bacillus subtilis* lipopeptides' fengycins against *Alternaria solani* in potato as assessed by a transcriptome analysis. Front Microbiol 13:861113

Zhao W, Chen HL, Hong L, Zhang X, Jiang XJ, Zhu DL, Wang F, Yang XL (2019) Five new polyphenolic derivatives with antimicrobial activities from the root barks of *Periploca sepium*. Fitoterapia 137:104254

Zhao WR, Subbiah V, Xie CD, Yang ZH, Shi LH, Barrow C, Dunshea F, Suleria HAR (2022) Bioaccessibility and bioavailability of phenolic compounds in seaweed. Food Rev Int 39(8):5729–5760